In Situ Raman Spectroscopy of Supported Transition Metal Oxide Catalysts: $^{18}O_2-^{16}O_2$ Isotopic Labeling Studies

Bert M. Weckhuysen*

Centrum voor Oppervlaktechemie en Katalyse, Departement Interfasechemie, K.U.Leuven, Kardinaal Mercierlaan 92, 3001 Leuven (Heverlee), Belgium

Jih-Mirn Jehng

Department of Chemical Engineering, National Chung-Hsing University, Taichung 402, Taiwan, R.O.C.

Israel E. Wachs

Zettlemoyer Center for Surface Studies, Department of Chemical Engineering, Lehigh University, 7 Asa Drive, Bethlehem, Pennsylvania, 18015

The isothermal isotopic exchange reaction of $^{18}O_2$ with ^{16}O of CrO_3, MoO_3, Nb_2O_5, WO_3, V_2O_5, and Re_2O_7 supported on ZrO_2 has been investigated with in situ laser Raman spectroscopy. Isotopic exchange of the oxygen atoms of the supported transition metal oxides with $^{18}O_2$ is difficult and requires several successive reduction$-^{18}O_2$ reoxidation cycles at relatively high temperatures. The Raman spectroscopy data reveal that all the supported transition metal oxides are present as a monooxo species on ZrO_2. This finding is consistent with the shifts calculated from the isotopic ratios for a simple diatomic oscillator, with the corresponding infrared spectra of the same catalysts and with the vibrational frequencies of several monooxo reference compounds. On this basis, coordination models of the molecular structures are proposed for CrO_3/ZrO_2, MoO_3/ZrO_2, Nb_2O_5/ZrO_2, WO_3/ZrO_2, V_2O_5/ZrO_2, and Re_2O_7/ZrO_2 catalysts under dehydrated conditions.

Introduction

Transition metal oxides supported on inorganic oxides play a crucial role as heterogeneous catalysts in chemical industries for the production of commodity chemicals and the removal of noxious compounds from the environment.[1−3] Examples are the dehydrogenation of alkanes over CrO_3/Al_2O_3 catalysts,[4] methathesis of olefins over Re_2O_7/Al_2O_3 catalysts[5] and the selective catalytic reduction of NO_x over V_2O_5/TiO_2 catalysts.[6] Different spectroscopic techniques, such as electron spin resonance (ESR), diffuse reflectance spectroscopy in the UV−vis−near-IR region (DRS), infrared spectroscopy (IR), X-ray absorption spectroscopy (EXAFS-XANES), and Raman spectroscopy (RS), have been extensively used in order to unravel the molecular structure of these catalysts.[7−22] Such characterization is far from easy because the transition metal ion (M) can be present on the surface in different coordination environments, oxidation states, and polymerization degrees. In this respect, in situ Raman spectroscopy is a very powerful characterization technique because it can discriminate between different molecular structures of a transition metal oxide on a surface and monitor the vibrational changes of supported metal oxide catalysts under catalytic conditions.[23−25] Such information is crucial for developing structure−activity relationships in the field of heterogeneous catalysis and for the elucidation of reaction mechanisms.

Although tremendous progress has been made in the past, the exact molecular structure of supported transition metal oxide catalysts under dehydrated conditions remains unclear. More
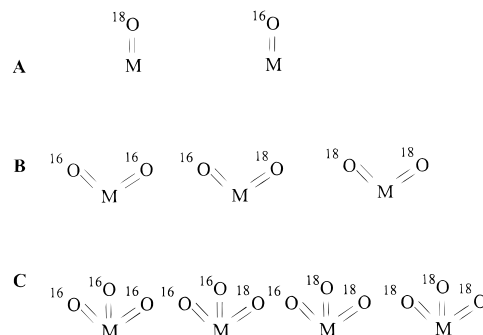
Figure 1. Molecular structure of a supported monooxo species (structure A), dioxo species (structure B), and trioxo species (structure C), and their corresponding ^{18}O-exchanged counterparts.

specifically, it is not yet clear how many terminal M=O bonds are present in these surface molecular entities; in other words, are the supported transition metal oxides present as a monooxo, a dioxo, or a trioxo species? An illustrative example is the limited knowledge about the molecular structure of supported rhenium oxide catalysts, which are generally considered to consist of isolated trioxo species of the type $S-O-Re(=O)_3$ species with S an oxygen atom of the inorganic oxide.[5]

The objective of the present investigation is to resolve this issue by combining in situ Raman spectroscopy with oxygen-18 isotopic labeling studies. Such studies allow obtaining fundamental information about the number of terminal M=O bonds and discriminating between monooxo, dioxo, and trioxo species. This is schematically illustrated in Figure 1. A monooxo species (structure A) should give rise to two Raman vibrations,

* To whom correspondence should be addressed. E-mail: Bert.Weckhuysen@agr.kuleuven.ac.be.

Spectra of Supported Transition Metal Oxide Catalysts

J. Phys. Chem. B, Vol. 104, No. 31, 2000 **7383**

M=^{16}O and M=^{18}O; a dioxo species (structure B) should exhibit three Raman vibrations, ^{16}O=M=^{16}O, ^{18}O=M=^{18}O, and ^{16}O=M=^{18}O; while a trioxo species (structure C) should give rise to four Raman vibrations, ^{16}O=M(=^{16}O)=^{16}O, ^{18}O=M(=^{16}O)=^{16}O, ^{18}O=M(=^{18}O)=^{16}O, and ^{18}O=M(=^{18}O)=^{18}O. It will be shown that vanadium(V) oxide, molybdenum(VI) oxide, niobium(V) oxide, tungsten(VI) oxide, chromium(VI) oxide, and rhenium(VII) oxide are all present as monooxo species at high metal oxide loading on a zirconia surface. This important finding is consistent with the isotopic shifts calculated from the isotopic ratios for a simple diatomic oscillator, with the corresponding infrared spectra of the same catalysts and with the vibrational frequencies of several monooxo reference compounds of the transition metal ions under study. On this basis, molecular structures are proposed for CrO_3/ZrO_2, MoO_3/ZrO_2, Nb_2O_5/ZrO_2, WO_3/ZrO_2, V_2O_5/ZrO_2, and Re_2O_7/ZrO_2 catalysts under dehydrated conditions.

Experimental Section

1. Catalyst Preparation and Characterization. Supported vanadium(V) oxide, molybdenum(VI) oxide, niobium(V) oxide, tungsten(VI) oxide, chromium(VI) oxide, and rhenium(VII) oxide catalysts have been prepared using ZrO_2 (Degussa, 39 m^2/g) as the support. The supported metal oxide catalysts under study are 6% CrO_3/ZrO_2, 4% MoO_3/ZrO_2, 5% Nb_2O_5/ZrO_2, 3% WO_3/ZrO_2, 4% V_2O_5/ZrO_2, and 3% Re_2O_7/ZrO_2 and details about these catalysts and their preparation can be found in previous publications.[8,18-21,26] The transition metal oxide loadings of these catalysts correspond with high coverages, but no crystalline phases were observed. Thus, well-dispersed supported transition metal oxides were studied in all cases. It has been shown previously that ZrO_2 has excellent characteristics for performing oxygen-18 isotopic labeling in combination with in situ Raman spectroscopy.[26] This is because this support is a weak Raman scatterer in the spectral region of interest (1100-700 cm^{-1}) and, as a consequence, does not obscure significantly the M=O and M-O-M vibrations. In addition, it does not show any fluorescence at high temperatures, which results in well-resolved Raman spectra and has a low surface area and therefore a relatively low number of reduction-reoxidation cycles for a significant isotopic exchange is required.

2. Raman Spectroscopy and Sample Treatment. Raman spectra of the supported metal oxide catalysts were obtained with a laser Raman apparatus with the 514.5 nm line of an Ar$^+$ laser (Spectra Physics, model 171) as the excitation source. The laser power at each sample was about 40 mW. The scattered radiation from the sample was directed into a Spex Triplemate spectrometer (model 1877) coupled to a Princeton Applied Research (model 1463) OMA III optical multichannel photodiode array detector (1024 pixels). The detector was cooled thermoelectronically to -35 °C to decrease the thermal noise. The Raman scattering in the 600-1100 cm^{-1} region was collected, and the spectra were recorded using an OMAIII computer and software. The instrument resolution was experimentally determined to be better than 2 cm^{-1}. About 0.2 g of each supported transition metal oxide catalyst was pressed into a thin film wafer of about 1 mm thickness. The catalyst samples were first calcined in dry air at 500 °C for 2 h in order to minimize possible sample fluorescence. The in situ Raman spectra were obtained according to the following procedure. The samples were placed in the cell and heated to 550 °C for 2 h in a flow of pure oxygen gas (Linde Specialty Grade, 99.99% purity). Flowing of pure $^{18}O_2$ gas (JWS Technologies, Inc., Matheson, and $^{18}O_2$/He ratio = 3/97) at different temperatures

TABLE 1: Observed Raman Bands before and after Reduction-Oxidation Cycles for the Supported Transition Metal Oxide Catalysts under Study

catalyst	pretreatment	experimentally observed Raman bands (cm^{-1})
6% CrO_3/ZrO_2	after calcination	1030; 1010; 880
	after successive reduction-oxidation cycles	1030; 1010; 880; 990; 970; 840
4% MoO_3/ZrO_2	after calcination	996; 850
	after successive reduction-oxidation cycles	996; 850; 950; broad unresolved Raman band
5% Nb_2O_5/ZrO_2	after calcination	980; 800
	after successive reduction-oxidation cycles	980; 800; 930; broad unresolved Raman band
3% WO_3/ZrO_2	after calcination	1005; 790
	after successive reduction-oxidation cycles	1002; 790; 950; 750
4% V_2O_5/ZrO_2	after calcination	1030; 920
	after successive reduction-oxidation cycles	1030; 920; 990; broad unresolved Raman band
3% Re_2O_7/ZrO_2	after calcination	1005; 890
	after successive reduction-oxidation cycles	1000; 882; 945; 840

resulted in only minor changes in the Raman spectra of the calcined catalysts and this method was not further exploited because of the inefficiency of the isotopic exchange reaction. Another method was developed in which either butane (Air Products and Chemicals, mixture of 98.7% He and 1.3% butane) or hydrogen gas (Linde Grade, 99.9% purity) was used for an initial reduction of the supported metal oxide catalysts. These gases were dynamically introduced into the cell at 450 °C, and Raman spectra were collected. These spectra did not show Raman features, indicating that the Raman cross sections of the reduced transition metal ions are too low to be experimentally observed. The reduced samples were then reoxidized in $^{18}O_2$ at 450 °C. This reduction-reoxidation cycle for each catalyst was repeated until the extent of oxygen-18 isotopic exchange clearly allowed to judge the number of M=O bonds from the Raman spectra. In a previous study,[26] we have observed that the maximum number of reduction-reoxidation cycles for complete isotopic exchange of the supported transition metal oxide decreases with increasing reduction and reoxidation temperature. The optimal reduction and reoxidation temperature was determined to be around 450 °C. The Raman spectra were deconvoluted with GRAMS/386 of Galactic Industries, Inc. It is important to stress that the Raman cross sections do not change upon oxygen-18 labeling. Therefore, the bandwidths and band shapes are constant and can be used to deconvolute the Raman spectra after successive oxygen-18 labeling. This allows us to determine the degree of oxygen exchange of the M=O bond. Unfortunately, it was not possible to determine the degree of the M-O-M bond because of difficulties in subtracting the support background and the broadness of the Raman band corresponding to this bond.

Results

Table 1 gives an overview of the observed Raman bands of the 6% CrO_3/ZrO_2, 4% MoO_3/ZrO_2, 5% Nb_2O_5/ZrO_2, 3% WO_3/ZrO_2, 4% V_2O_5/ZrO_2, and 3% Re_2O_7/ZrO_2 catalysts after calcination in $^{16}O_2$ at 550 °C and after successive reduction-reoxidation cycles at 450 °C with $^{18}O_2$. In accordance with

Figure 2. In situ Raman spectra of the dehydrated 3% Re_2O_7/ZrO_2 catalyst as a function of the number of oxidation−reduction cycles with $^{18}O_2$.

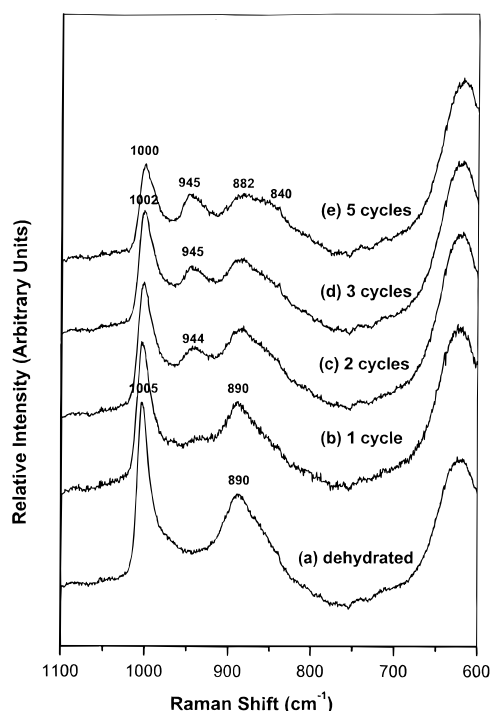**Figure 3.** In situ Raman spectra of the dehydrated 5% Nb_2O_5/ZrO_2 catalyst as a function of the number of oxidation−reduction cycles with $^{18}O_2$.

previous papers,[18−24] the Raman bands of the supported metal oxide catalysts obtained after calcination in $^{16}O_2$ at 550 °C in the range between 1050 and 950 cm^{-1} can be unambiguously assigned to the symmetric stretching mode of short terminal M=O bonds (i.e., $\nu_s[M=O]$), whereas Raman bands in the range between 750 and 950 cm^{-1} are attributed to either the antisymmetric stretch of M−O−M bonds (i.e., $\nu_{as}[M-O-M]$) or the symmetric stretch of $(-O-M-O-)_n$ bonds (i.e., $\nu_s[(-O-M-O-)_n]$). Isotopic substitution of ^{16}O for ^{18}O does not appreciably affect the internuclear distance in the M=O or M−O−M bonds, but there is a change in total mass, which results in a systematic shift of the Raman bands to lower frequency after successive reduction−reoxidation cycles with $^{18}O_2$ (Table 1). Both the number of new Raman bands formed and the shift to lower frequency are dependent on the initial molecular structures of the supported transition metal oxides. It is this information which is exploited in this paper for discriminating between monooxo, dioxo, and trioxo surface species.

As an example, we will discuss the in situ Raman spectra of the Re_2O_7/ZrO_2, Nb_2O_5/ZrO_2, and WO_3/ZrO_2 catalysts in detail, but similar observations were made for the other supported transition metal oxide catalysts. Figure 2 shows the in situ Raman spectra of the 3% Re_2O_7/ZrO_2 catalyst obtained after calcination and after successive reduction−reoxidation cycles. The spectrum of the calcined 3% Re_2O_7/ZrO_2 catalyst is characterized by an intense $\nu_s[Re=O]$ vibration at 1005 cm^{-1} and a broader $\nu_{as}[Re-O-Re]$ vibration at around 890 cm^{-1}. After calcination at 550 °C in oxygen for 2 h, the catalyst sample was cooled and contacted with hydrogen at 450 °C for 0.5 h and reoxidized at this temperature with $^{18}O_2$. The corresponding spectrum is included in Figure 2. The Raman band at 1005 cm^{-1} is decreased in intensity at the expense of a weak scattering at around 945 cm^{-1}. In addition, the band at 890 cm^{-1} broadens toward lower frequency. After repeating this reduction−reoxidation cycle five times, the Raman spectra change drastically, as illustrated in Figure 2. The following observations can be made: (1) the intensity of the 1005 cm^{-1} band further
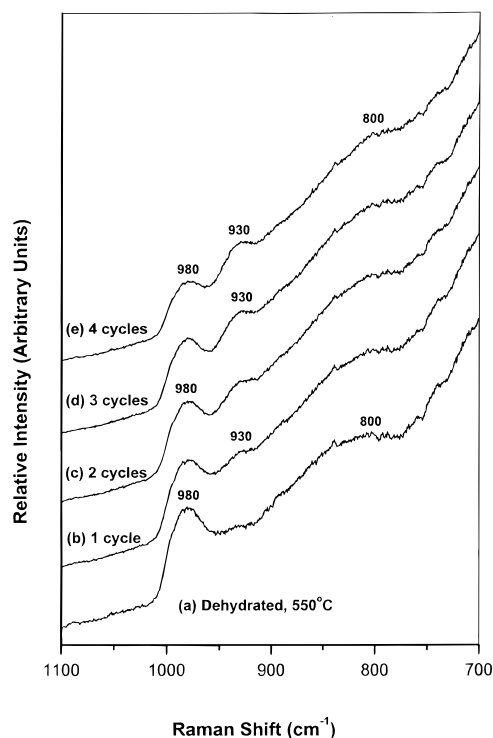
decreases to only 50% of its original intensity; (2) the Raman band at 1005 cm^{-1} slighly shifts to lower frequency; (3) a new Raman band at 945 cm^{-1} is formed; (4) the Raman band at 890 cm^{-1} decreases in intensity and shifts to 882 cm^{-1}; and (5) a new Raman band at around 840 cm^{-1} is formed. It appears that only two new Raman bands at 945 and 840 cm^{-1} are formed at the expense of the 1005 and 890 cm^{-1} Raman bands. No other Raman bands are formed by oxygen-18 isotope exchange of these catalysts.

The in situ Raman spectra of the 5% Nb_2O_5/ZrO_2 catalyst obtained after calcination and after successive reduction−reoxidation cycles are given in Figure 3. The spectrum of the calcined 5% Nb_2O_5/ZrO_2 catalyst is characterized by an intense Raman active $\nu_s[Nb=O]$ vibration at 980 cm^{-1} and a broad ill-resolved Raman active $\nu_{as}[Nb-O-Nb]$) vibration at 800 cm^{-1}. Four successive reduction−reoxidation cycles of the 5% Nb_2O_5/ZrO_2 catalyst at 450 °C resulted in important changes in the Raman spectra. These spectral changes can be summarized as follows: (1) The intensity of the 980 cm^{-1} Raman band decreases with increasing number of reduction−reoxidation cycles to 40% of its original intensity; (2) A new Raman band at 930 cm^{-1} is formed; and (3) the Raman band at 800 cm^{-1} further broadens and becomes ill-defined. It appears again that the new Raman band at 930 cm^{-1} is formed at the expense of the 980 cm^{-1} Raman band and that no other Raman bands are formed in this region during oxygen-18 isotopic labeling.

Figure 4 shows the in situ Raman spectra of the 3% WO_3/ZrO_2 catalyst obtained after calcination and after successive reduction−reoxidation cycles. The spectrum of the calcined 3% WO_3/ZrO_2 catalyst is characterized by a strong Raman active $\nu_s[W=O]$ vibration band at 1005 cm^{-1} and a broad Raman active $\nu_{as}[W-O-W]$) band at around 790 cm^{-1}. The catalyst sample was then cooled and contacted with hydrogen at 450 °C for 0.5 h and reoxidized at the same temperature with $^{18}O_2$. The corresponding spectrum is included in Figure 4. The Raman band at 1005 cm^{-1} is decreased in intensity at the expense of a
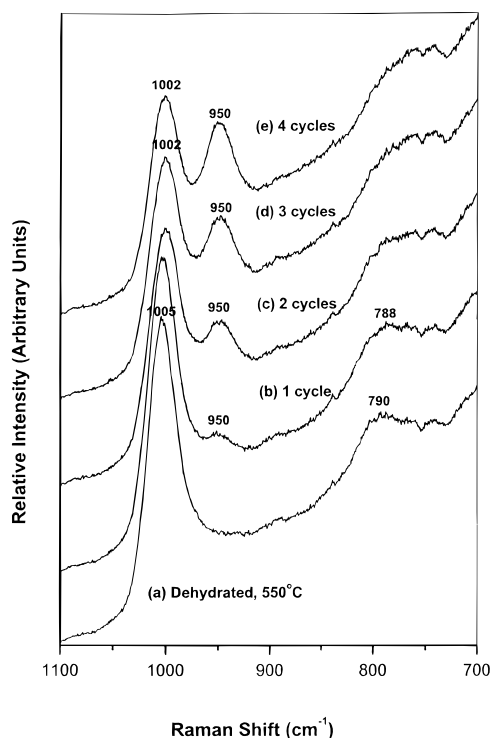
Spectra of Supported Transition Metal Oxide Catalysts

J. Phys. Chem. B, Vol. 104, No. 31, 2000 **7385**

Figure 4. In situ Raman spectra of the dehydrated 3% WO_3/ZrO_2 catalyst as a function of the number of oxidation−reduction cycles with $^{18}O_2$.

weak Raman band at around 950 cm^{-1}. After repeating this reduction−reoxidation cycle four times, the Raman spectra change drastically, as illustrated in Figure 4. These changes can be summarized as follows: (1) the intensity of the 1005 cm^{-1} band further decreases to 60% of its original intensity with increasing number of reduction−reoxidation cyles; (2) the Raman band at 1005 cm^{-1} slighly shifts to 1002 cm^{-1}; (3) a new Raman band at 950 cm^{-1} is formed; and[4] the Raman band at 790 cm^{-1} shifts to lower frequency and becomes broader. It can be concluded that that the new Raman band at 950 cm^{-1} is formed at the expense of the 1005 cm^{-1} Raman band and that no other Raman bands are formed in this region from the oxygen-18 isotope exchange.

Similar observations were made for the 6% CrO_3/ZrO_2, 4% MoO_3/ZrO_2, and 4% V_2O_5/ZrO_2 catalysts. The in situ Raman spectra of the 4% MoO_3/ZrO_2 and 4% V_2O_5/ZrO_2 catalysts indicate that after successive reduction−reoxidation cycles with $^{18}O_2$ only one new Raman band is formed at the expense of the Raman-active $\nu[M=O]$ vibration band initially observed in the Raman spectrum of the calcined catalysts (Table 1). The situation is more complex for the 6% CrO_3/ZrO_2 catalyst because two different chromium oxide species are present after calcination; i.e., a polymeric species and a monomeric species, which both undergo oxygen-18 isotopic exchange after successive reduction−reoxidation cycles with $^{18}O_2$. A detailed discussion of the corresponding in situ Raman spectra has already been given in a previous paper[26] and will not be repeated here. The conclusion was that for each Raman active $\nu[Cr=O]$ vibration band, belonging to either the monomeric or polymeric chromium oxide species, a new Raman band was formed with a frequency about 40 cm^{-1} lower than that of the initially observed Raman band (Table 1).

Finally, the small shifts of the $M=O$ and $M-O-M$ bond frequencies have to be addressed. The only explanation we can envisage for the shifts of the $M=O$ Raman frequency observed for the Re_2O_7/ZrO_2 and WO_3/ZrO_2 catalysts is that there is some

residual moisture on the catalyst bed after successive reduction−reoxidation cycles. This moisture may result in small shifts toward lower wavenumber. On the other hand, the small shifts observed for the $M-O-M$ bond Raman frequencies of the supported metal oxide catalysts are less certain because of possible changes in the support background. It is difficult to give at this moment a reasonable explanation for these shifts, although we do not believe that the structure of the surface metal oxide species change during the reduction−reoxidation cycles.

Discussion

The present oxygen-18 isotopic exchange experiments provide fundamental information about the number of $M=O$ bonds present in the supported vanadium oxide, rhenium oxide, tungsten oxide, niobium oxide, chromium oxide, and molybdenum oxide catalysts. As was already pointed out in the Introduction, this information allows us discriminate between monooxo, dioxo, and trioxo species supported on the zirconia surface as schematically illustrated in Figure 1. A monooxo species (structure A) should give rise to two strong Raman vibrations ($M=^{16}O$ and $M=^{18}O$), a dioxo species (structure B) should exhibit three strong Raman vibrations ($^{16}O=M=^{16}O$, $^{18}O=M=^{18}O$, and $^{16}O=M=^{18}O$), while a trioxo species (structure C) should give rise to four strong Raman vibrations ($^{16}O=M(=^{16}O)=^{16}O$, $^{18}O=M(=^{16}O)=^{16}O$, $^{18}O=M(=^{18}O)=^{16}O$, and $^{18}O=M(=^{18}O)=^{18}O$).[27,28]

All the spectroscopic results presented in this study point toward the same conclusion; i.e., the presence of monooxo species in the supported transition metal oxide catalysts under dehydrated conditions. Indeed, it can be concluded that the intensity of only one Raman active $\nu_s[M=^{18}O]$ vibration gradually increases at the expense of the intensity of the Raman active $\nu_s[M=^{16}O]$ vibration and that no other Raman vibrations (eventually arising from the presence of a dioxo or trioxo species) could be observed after isotopic labeling with $^{18}O_2$.

Furthermore, a Raman band characteristic of a simple $M-O$ diatomic oscillator will lead to an isotopic ratio:[27,28]

isotopic ratio =

$$\left[\frac{\nu^{16}_{O-M}}{\nu^{18}_{O-M}} \right] = \frac{\frac{1}{2\pi c}\sqrt{k\left(\frac{1}{m_M}+\frac{1}{m_{16}}\right)}}{\frac{1}{2\pi c}\sqrt{k\left(\frac{1}{m_M}+\frac{1}{m_{18}}\right)}} = \frac{\sqrt{\left(\frac{1}{m_M}+\frac{1}{m_{16}}\right)}}{\sqrt{\left(\frac{1}{m_M}+\frac{1}{m_{18}}\right)}}$$

with ν the frequency of the $M-O$ bond (cm^{-1}), k the force constant, and m the mass of the transition metal ion or oxygen. The calculated values are given in Table 2. For example, a $W-O$ diatomic oscillator has an isotopic ratio of 1.0554. This ratio allows us to calculate the theoretical isotopic shifts for the experimentally Raman bands at 1005 and 790 cm^{-1} observed before isotopic labeling. The theoretical Raman bands after isotopic exchange with $^{18}O_2$ are located at 952 and 749 cm^{-1}, which corresponds very well with the experimentally observed Raman peaks at 950 and 750 cm^{-1}. Thus, there exist an excellent agreement between the theoretically calculated and experimentally observed isotopic shifts for the supported transition metal oxide catalysts (Table 2). One could always argue that if the bond angle in a MO_2 group is near 90° and for an appropriate interaction force constant between the two $M=O$ groups, then only one new Raman band would be observed for oxygen-18 isotope exchange supported transition metal oxide catalysts. However, it seems rather unlikely that this would take place for the supported vanadium oxide, rhenium oxide, tungsten oxide, niobium oxide, chromium oxide, and molybdenum oxide catalysts at the same time.

TABLE 2: Isotopic Ratios, Together with the Experimentally Observed and Theoretically Calculated Raman Shifts for the Supported Transition Metal Oxide Catalysts[a]

transition metal ion (M)	isotopic ratio	M=O bond (cm^{-1})			M−O−M or (O−M−O)$_n$ bond (cm^{-1})		
		[M=^{16}O]$_e$	[M=^{18}O]$_e$	[M=^{18}O]$_t$	[M−^{16}O−M]$_e$	[M−^{18}O−M]$_e$	[M−^{18}O−M]$_t$
Cr	1.0454	1030	990	985	880	840	842
Mo	1.0513	996	950	947	850	nr	808
Nb	1.0510	980	930	932	800	nr	761
W	1.0554	1005	950	952	790	750	749
V	1.0452	1030	990	985	920	nr	880
Re	1.0555	1005	945	952	882	840	836

[a] nr = not resolved; e = experimentally observed; t = theoretically calculated.

TABLE 3: Comparison between Raman (RS) and Infrared (IR) Band Positions for the Supported Transition Metal Oxide Catalysts

vibration (cm^{-1})	Cr		Mo		Nb		W		V		Re	
	RS	IR	RS	IR	RS	IR	RS	IR	RS	IR	RS	IR
ν_s[M=O]	1030	1030	996	885	980	986	1005	1004	1030	1028	1005	1003
	1010	1010										
ν_{as}[M−O−M] or ν_s[(O−M−O)$_n$]	880	875	850	845	930	925	790	no	920	922	890	no

[a] no = not experimentally observed.

TABLE 4: Survey of the Monooxo Reference Compounds of Cr(VI), V(V), W(VI), Nb(V), Mo(VI), and Re(VII) Formed with Halides (29) and, if Already Reported in the Literature, Their Corresponding Vibrational Frequencies of the M=O Bond[a]

monooxo reference compound	vibrational freq of the M=O bond (cm^{-1})	ref
F$_4$Cr=O	1028	31
F$_3$V=O	1058	29
Cl$_3$V=O	1035	29
Br$_3$V=O	1025	29
F$_4$W=O	1055	27
Cl$_4$W=O	nr	-
Br$_4$W=O	nr	-
Cl$_3$Nb=O	997	27
Br$_3$Nb=O	nr	-
I$_3$Nb=O	nr	-
F$_4$Mo=O	1039	32
Cl$_4$Mo=O	1008	33
F$_5$Re=O	990	27

[a] nr = not reported in the literature.

Additional evidence for the proposal of the monooxo structure for supported transition metal oxide catalysts can be found in a comparison between in situ Raman and infrared data obtained for the same catalysts under dehydrated conditions. Such comparison is made in Table 3. Indeed, the presence of only one vibration will indicate a monooxo species because a diatomic oscillating system has only one stretching mode (ν_s), while in the case of a dioxo species two bands due to the symmetric (ν_s) and antisymmetric (ν_{as}) stretching modes of this triatomic system will be visible.[27,28] These frequencies should be separated by about 10−30 cm^{-1}. Furthermore, for the dioxo species the symmetric mode will be more intense in Raman, while the antisymmetric mode will dominate in IR. Based on the coincident frequency of the IR and Raman frequencies in Table 3, it appears that the supported transition metal oxides are all present as monooxo species. The presence of these monooxo species for Cr(VI), V(V), W(VI), Nb(V), Mo(VI), and Re(VII) oxides supported on a zirconia surface under dehydrated conditions may not wonder in view of the several Cr(VI), V(V), W(VI), Nb(V), Mo(VI), and Re(VII) oxohalide compounds already reported in the literature.[29] A survey of these compounds is given in Table 4. It is clear that many monooxo compounds exist for W(VI), Mo(VI), Nb(V), and V(V) oxohalides. This is not the case for Cr(VI) and Re(VII), which form only a monooxo

compound with the most electronegative halide F$^-$. Dioxo and trioxo Cr(VI) and Re(VII) oxohalides are much more frequently encountered in nature; i.e., CrO$_2$F$_2$, CrO$_2$Cl$_2$, CrO$_2$Br$_2$, ReO$_2$F$_2$, ReO$_3$F, ReO$_3$Cl, ReO$_3$Br.[29] This scarcity of monooxo compounds for Cr(VI) and Re(VII) in nature may explain why such a structure has not been proposed in the past for supported chromium oxide and rhenium oxide catalysts.

Finally, it is important to recall that during dehydration the surface transition metal oxide species change their molecular structures and the transition metal ions become highly distorted on the surface upon anchoring with the hydroxyl groups of the support. This distortion results in the formation of very short monooxo terminal M=O bonds, which vibrate around or above 1000 cm^{-1}. Such frequencies are in line with those already observed by vibrational spectroscopies for the monooxo reference compounds of Table 4.[30−33] This strongly indicates that such high Raman vibrations can indeed be attributed, independent of the polymerization degree, to a monooxo species supported on an inorganic surface. The presence of monooxo species is also revealed in combination of IR spectroscopy and oxygen-18 isotopic exchange experiments in Cr$_2$O$_3$,[34] SO$_4$/Al$_2$O$_3$,[35] and SO$_4$/TiO$_2$.[35]

The present data allow us to propose models for the molecular structures of CrO$_3$, MoO$_3$, Nb$_2$O$_5$, WO$_3$, V$_2$O$_5$, and Re$_2$O$_7$ present at high loadings on zirconia surfaces under dehydrated conditions. This is illustrated in Figure 5 and the experimentally observed vibrational frequencies belonging to the different molecular bonds of these models are included. All the model structures presented are electronically neutral because each double bond with oxygen delivers two negative formal charges and each single bond with oxygen delivers one negative formal charge to the transition metal cation. These covalent bondings allow the transition metal cation to distribute its very high positive charge between 5 (e.g., Nb^{5+} or V^{5+}) and 7 (e.g., Re^{7+}) over the molecular entity in molecular orbitals and consequently drastically lowers its formal positive charge.

CrO$_3$ on ZrO$_2$ under dehydrated conditions can be either present as an isolated or a polymeric species, but both possess a monooxo structure. The isolated monooxo species are characterized by Raman bands at 1030 cm^{-1}, while the polymeric monooxo species is characterized by Raman bands at 1010 and 880 cm^{-1}. It has been shown in a previous publication that this polymeric species is much more easily to
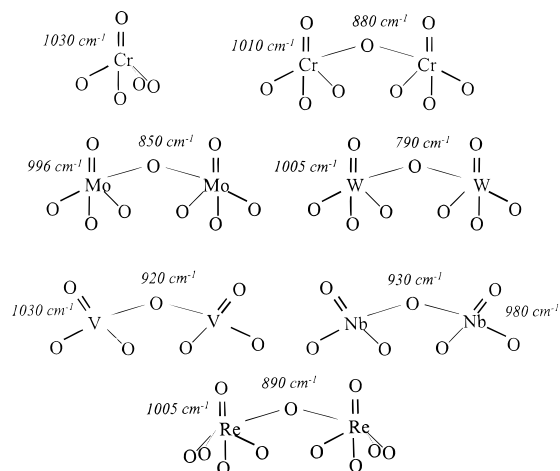
Spectra of Supported Transition Metal Oxide Catalysts

J. Phys. Chem. B, Vol. 104, No. 31, 2000 **7387**

Figure 5. Schematic drawing of the molecular structures of CrO_3, MoO_3, Nb_2O_5, WO_3, V_2O_5, and Re_2O_7 present at high metal oxide loadings on zirconia surfaces under dehydrated conditions, including the observed vibrational frequencies belonging to the molecular bonds.

reduce with butane at high temperatures than the monomeric monooxo species.[36] On the other hand, MoO_3 on ZrO_2 is present as a polymeric monooxo species with Raman vibrations at 996 and 850 cm^{-1}, and Mo has in this model a formal coordination number of 5, which is close to a distorted octahedral coordination. Similar structures can be envisaged for WO_3. The models of Nb_2O_5 and V_2O_5 on ZrO_2 are also very similar (Figure 5). Here, a polymeric species is formed with V or Nb in a pseudo-tetrahedral coordination, giving rise to Raman vibrations for V_2O_5 at 1030 and 920 cm^{-1}. The coordination model for Re_2O_7 on ZrO_2 can be best envisaged as a polymeric species, in which at least two octahedron-like coordinated Re^{7+} atoms are linked together via an oxygen atom. The coordination sphere of each rhenium atom is completed by four oxygen atoms of the zirconia support. Such model has been never been postulated before in the literature but is consistent with the reported data in this paper.

Conclusions

In situ laser Raman spectroscopy in combination with oxygen-18 labeling studies is a powerful technique for the elucidation of the molecular structure of supported transition metal oxide catalysts under dehydrated conditions because it allows to discriminate between monooxo, dioxo and trioxo species. The present investigation reveals that the supported CrO_3, MoO_3, Nb_2O_5, WO_3, V_2O_5, and Re_2O_7 on zirconia all possess, independent of their polymerization degree, a monooxo structure under dehydrated conditions. This important but partially unexpected finding is consistent with the shifts calculated from the isotopic ratios for a simple diatomic oscillator, with the corresponding infrared spectra of the same catalysts and with the vibrational frequencies of several monooxo reference compounds.

The present Raman data also rejects the classical hypothesis for the molecular structure of supported rhenium oxide catalysts, which assumed an isolated trioxo species of the type S−O−Re(=O)$_3$ species with S an oxygen atom of the inorganic oxide. Instead, the molecular structure of supported rhenium oxide catalysts is better described by a polymeric species, in which

at least two octahedron-like coordinated Re^{7+} are linked together via an oxygen atom. To our best knowledge, this is the second example, in which Re(VII) is known to be present in a chemical compound as a monooxo structure.

References and Notes

(1) Thomas, J. M.; Thomas, W. J. *Principles and practice of heterogeneous catalysis;* VCH: Weinheim, Germany, 1997.

(2) Ertl, G., Knozinger, H., Weitkamp, J., Eds. *Handbook of Heterogeneous Catalysis*; Wiley-VCH: Weinheim, Germany, 1997.

(3) Wachs, I. E., Ed. Applications of supported metal oxide catalysts. *Catal. Today* **1999**, *51*, 201−348 (special issue).

(4) Weckhuysen, B. M.; Schoonheydt, R. A. *Catal. Today* **1999**, *51*, 223.

(5) Mol, J. C. *Catal. Today* **1999**, *51*, 289.

(6) Bosh, H.; Janssen, F. J. J. G. *Catal. Today* **1988**, *2*, 369.

(7) Indovina, V. *Catal. Today* **1998**, *41*, 95.

(8) Deo, G.; Wachs, I. E. *J. Phys. Chem.* **1991**, *95*, 5889.

(9) Hercules, D. M.; Proctor, A.; Houalla, M. *Acc. Chem. Res.* **1994**, *27*, 387.

(10) Reddy, B. M.; Chowdury, B.; Ganesh, I.; Reddy, E. P.; Rojas, T. C.; Fernandez, A. *J. Phys. Chem. B* **1998**, *102*, 10176.

(11) Prinetto, F.; Ghiotti, G.; Occhiuzi, M.; Indovina, V. *J. Phys. Chem. B* **1998**, *102*, 10316.

(12) Takenaka, S.; Tanaka, T.; Funabiki, T.; Yoshida, S. *J. Phys. Chem. B* **1998**, *102*, 2960.

(13) Whittington, B. I.; Anderson, J. R. *J. Phys. Chem.* **1993**, *97*, 1032.

(14) Chary, K. V. R.; Bhaskar, T.; Krishan, G.; Vijayaumar, V. *J. Phys. Chem. B* **1998**, *102*, 3936.

(15) Gao, X.; Bare, S. R.; Fierro, J. L. G.; Wachs, I. E. *J. Phys. Chem. B* **1999**, *103*, 618.

(16) Arena, F.; Frusteri, F.; Parmaliana, A. *Appl. Catal. A: General* **1999**, *176*, 189.

(17) Sharf, U.; Shraml-Marth, M.; Wokaun, A.; Baiker, A. *J. Chem. Soc., Faraday Trans.* **1991**, *87*, 3299.

(18) Vuurman, M. A.; Wachs, I. E.; Stufkens, D. J.; Oskam, A. *J. Mol. Catal.* **1993**, *80*, 209.

(19) Burcham, L. J.; Datka, J.; Wachs, I. E. *J. Phys. Chem. B* **1999**, *103*, 6015.

(20) Vuurman, M. A.; Wachs, I. E. *J. Phys. Chem.* **1992**, *96*, 5008.

(21) Kim, D. S.; Ostromecki, M.; Wachs, I. E. *J. Mol. Catal. A: Chem.* **1996**, *106*, 93.

(22) Mestl, G.; Srinivasan, T. K. K. *Catal. Rev. Sci. Eng.* **1998**, *40*, 451.

(23) Wachs, I. E. *Top. Catal.* **1999**, *8*, 57.

(24) Knozinger, H.; Mestl, G. *Top. Catal.* **1999**, *8*, 45.

(25) Wachs, I. E. in *Handbook of Raman Spectroscopy*; Marcel Dekker: New York, in press.

(26) Weckhuysen, B. M.; Wachs, I. E. *J. Phys. Chem. B* **1997**, *101*, 2793.

(27) Nakomoto, K. *Infrared and Raman spectra of Inorganic and Coordination Compounds*, 5th ed.; Wiley: New York, 1997.

(28) Banwell, C. N. *Fundamentals of Molecular Spectroscopy*, 3rd ed.; McGraw-Hill: London, 1983.

(29) Greenwood, N. N.; Earnshaw, A., *Chemistry of the Elements*; Pergamon Press: Oxford, UK, 1984.

(30) Hardcastle, F. D.; Wachs, I. E. *J. Phys. Chem.* **1991**, *95*, 5031.

(31) Cieslak-Golonka, M. *Coord. Chem. Rev.* **1991**, *109*, 223.

(32) Alexander, L. E.; Beattie, I. R.; Bukovsky, A.; Jones, P. J.; Marsden, C. J.; van Schalkwyk, *J. Chem. Soc., Dalton Trans.* **1974**, *81*, 74. Paine, R. T.; McDowell. *Inorg. Chem.* **1974**, *13*, 2366.

(33) Colin, R. J.; Griffith, W. P.; Pawson, D. *J. Mol. Struct.* **1973**, *19*, 531.

(34) Carrot, P. J. M.; Sheppard, N. *J. Chem. Soc., Faraday Trans. 1* **1983**, *79*, 2425.

(35) Saur, O.; Bensitel, M.; Mohammed Saad, A. B.; Lavalley, J. C.; Tripp, C. P.; Morrow, B. A. *J. Catal.* **1986**, *99*, 104.

(36) Weckhuysen, B. M.; Wachs, I. E. *J. Phys. Chem.* **1996**, *100*, 14437.